Application of Swarm Intelligence for the Multi-Objective Optimization of the Thermodynamic Performance and Economic of Double Reheat Steam Power Plants

Somboon Sukpancharoen[1*]

[1*]*Division of Mechatronics and Robotics Engineering, Rajamangala University of Technology Thanyaburi, Pathum Thani 12110, Thailand*

*Corresponding Author. E-mail address: somboon_s@rmutt.ac.th

Received: 23 March 2021; Revised: 4 May 2021; Accepted: 10 May 2021
Published online: 25 June 2021

Abstract

This paper seeks to employ swarm intelligence (SI) based algorithms to perform the multi-objective optimization of a steam power plant using double reheat and feedwater heaters. The analysis is carried out to take into consideration the 3E aspects of energy, exergy, and economy. The first and second laws of thermodynamics are applied in the analysis of the cycle and the optimization of both the thermal and exergy efficiencies. Assessment of the economic aspect involves consideration of the fixed and operating costs. Three SI algorithm were tested and the resulting system performance improvements in terms of 3E analysis were compared. The algorithms were the sparrow search algorithm (SSA), artificial jellyfish search (JS) optimizer, and cooperation search algorithm (CSA). The testing revealed that the SSA method approach offered the best search potential at the optimal cost, thus proving more economical than either of the alternative algorithms. Furthermore, when comparing the SSA method multi-objective optimization in the steam power plant with the based case, the respective improvements in thermal and exergy efficiency were from 48.9% to 49.54%, and from 46.13% to 48.06%, while the overall cost saving was 25.8%.

Keywords: Energy exergy and economic (3E) analysis, Thermodynamics modelling, Multi-objective optimization, Steam power plant, Swarm intelligence (SI)

I. INTRODUCTION

Electricity is generated all over the world using coal, oil, or natural gas as the fuel to produce the steam required for the process. The rate of energy consumption in the different countries worldwide can be used as an indicator that shows how developed those countries and the standard of living they have achieved [1].

The generation of electricity involves the conversion of one form of energy into another, and the total amount generated is currently trending upwards with annual global increases of about 2% to 3%. By 2030, it is anticipated that the total amount of electrical production will reach 30.3 billion kWh. The costs involved in this production will ultimately depend on the fuel used in the process and the power plant efficiency. For this reason, the cost function for a power plant will be defined in terms of the cost function for the fuel source involved [2].

To improve the operation of a power plant in terms of thermal efficiency, it is appropriate to begin by examining the feedwater heater network to create a more efficient design [3]. Much of the previous work has focused on applications of the first law of thermodynamics while disregarding the idea of irreversibility. Later studies have built upon that foundation by applying techniques based on equal enthalpy and temperature rises when designing the networks for the feedwater heaters [4]. This approach requires each heater to be designed independently before being added to the network of heaters. By integrating the feedwater heater design, the efficiency is greatly improved compared to conventional approaches, and it can be anticipated that the overall power plant thermal efficiency will also be enhanced as a result [2], [5].

Various techniques can be used to improve thermodynamic system efficiency. In particular, it can be helpful to make adjustments to how to input heat interacts with the performance of mechanical work to manipulate the total energy loss within the system. The first law of thermodynamics or the principle of energy conservation is relevant here, in particular, because the form of energy involved is not significant. While the balance of energy adheres to the first law, however, heat and work differ in qualitative terms. Therefore, it is not appropriate to assess a thermodynamic system solely from a quantitative perspective if the efficiency is determined. Instead, the second law of thermodynamics must also be taken into consideration. This is the concept of exergy, and it allows the quality of the energy to be evaluated. Moreover, it is also possible to calculate irreversibility through this approach, as well as determining the level of useful energy. In summary, although it is possible to analyze pressure and temperature and their effects within the system using the first law, irreversibility is assessed using the exergy method. Finally, the extent to which economic value is linked to exergy can also be established [6].

When energy conversion systems undergo performance evaluations, energy analysis has typically been the most common approach employed, but more recently exergy utilization and destruction have drawn increasing attention [7]. Energy systems can be considered in terms of exergy analysis, while from an economic perspective, it is possible to use exergo-economic analysis, which is an engineering field that draws upon elements of exergy analysis in combination with economic theory [8]. For a broad analysis of thermal power plants covering different viewpoints, one of the most effective means of assessing performance is through 3E analysis (energy, exergy, and environmental) [9], [10].

In one such example, Lee et al. [11] studied the pure refrigeration cycle in the process of natural gas

liquefaction and sought to minimize the energy by focusing attention upon the system for subcooling and conducting thermodynamic analysis upon the upgrade. Based on this analysis, the design underwent optimization to minimize the consumption of energy by determining the ideal pressure, temperature, flow rate, and compression ratio. Having optimized the parameters of the system it was possible to reduce the consumption of energy by 17.74%.

An exergo-economic power plant analysis was conducted by Rosen and Dincer [12] with a specific focus on a coal-fired power station. This study determined that it is essential to consider the relationship between capital costs and thermodynamic loss [10], [12].

Oyedepo et al. [13] reported that it is possible to improve the Rankine cycle performance while minimizing the fuel consumption by altering the design to feature closed feedwater heaters. If the number of feedwater heaters is increased, it has been shown that the heat rate and fuel consumption will decline, along with the heat rejected in the condenser and the heat input to the cycle.

A reheat Rankine cycle steam power plant underwent thermodynamic analysis by Rashidi et al. The plant contained six feedwater heaters, of which three were high pressure and three were low pressure, where deaeration is performed. The application of the first and second laws of thermodynamics permitted the maximization of the first and second law efficiencies [1].

Engineers developing the equipment and operational processes for power plants are obliged to perform a number of thermodynamic calculations in mechanical and chemical engineering scenarios. Furthermore, it is necessary to use the repeated solutions of problems based on thermal efficiency and exergy efficiency when designing the systems and their operating parameters. There is a high degree of complexity in these calculations due to the non-linear aspects of the thermodynamic models that explain the balance of mass, energy, and exergy, the potential nonconvexity of the objective thermodynamic functions, and the existence within the search space of trivial solutions. Such problems can be addressed using global optimization algorithms, which is an important field of study. One particular challenge is that the global minimum is often quite similar to local minima, and therefore global optimizers are particularly important [14].

One way to find solutions that are simultaneously optimized for a number of criteria is the multi-objective optimization approach [15], [16]. The optimization process can consider several different criteria; thermodynamic and economic factors must be taken into account, but it is important to note that if the focus is placed upon just one of these, the others may underperform to the detriment of the system. Only through simultaneous optimization can an advantageous outcome be obtained [17].

The complexity involved in designing optimal systems leads to the failure of conventional approaches to optimization. Such techniques tend to be lacking in efficiency or accuracy, and therefore it is necessary to develop novel optimization techniques that make use of artificial intelligence (AI) to quickly and accurately obtain global optima [18]–[21].

Rankine cycle optimization was studied by Elahifar et al. [2], who sought to maximize exergy efficiency. Some different algorithms were employed such as bee algorithm, firefly algorithm (FA), and teaching-learning-based (TLBO) optimization, with various parameters selected to serve as decision variables. The findings revealed that it is possible to improve exergy efficiency for the thermal power plant under investigation from 30.1% to 30.68%, 30.70368%, and 30.70369%, for each of the respective algorithms.

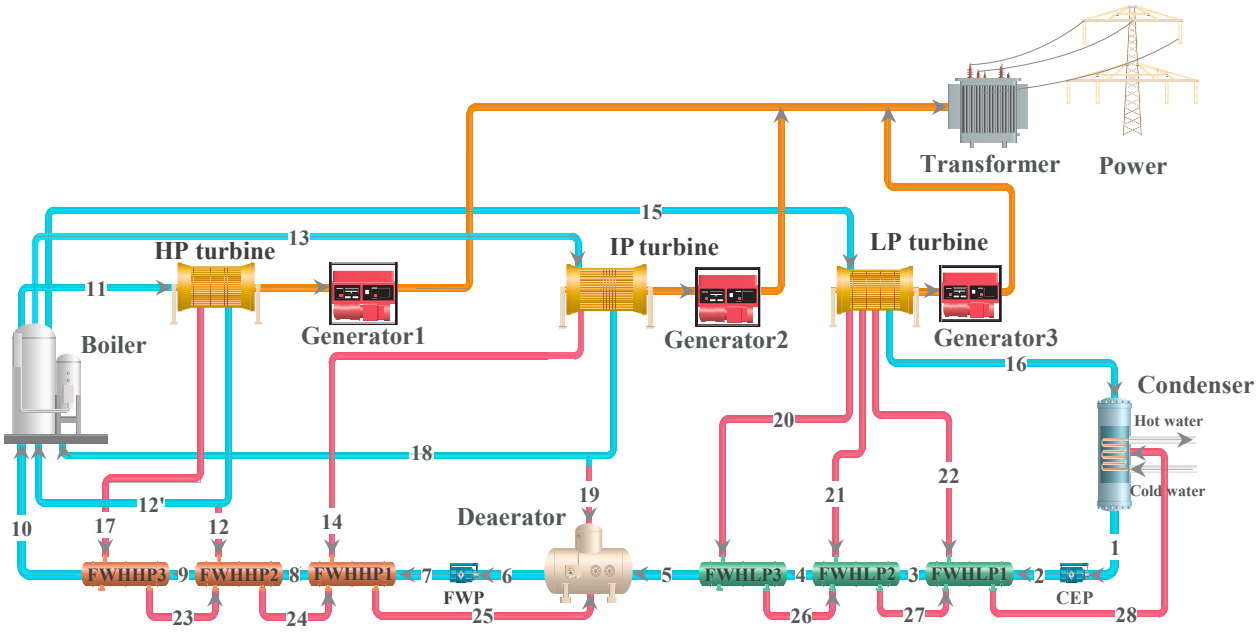

Figure 1 Schematic diagram showing the cycle of the double reheat steam power plant

One of the more effective optimization approaches is SI algorithm, which is based on the group behaviour patterns that result when individual members engage with their local environment. Functional global patterns are developed in such scenarios [21]. The SI algorithms which have been most widely applied to date include ant colony optimization (ACO) [22] and particle swarm optimization (PSO) [23].

However, while these algorithms have been relatively effective, the latest algorithms to be developed have shown even greater promise in analysing thermodynamic systems. These include the sparrow search algorithm (SSA) [24], Artificial Jellyfish Search (JS) optimizer [25], and Co-operation Search Algorithm (CSA) [26]. Therefore, this paper seeks to examine these latest algorithms in thermodynamic system analysis, like thermal efficiency, exergy efficiency, and economical cost, to optimize the system's performance and compare the effectiveness of the algorithms in achieving their results.

II. METHODOLOGY

A. Procedure depiction for the steam power plant using double reheat and feedwater heaters

The cycle flow sheet for the steam power plant from a previous study by Rashidi et al. [1] is presented in Figure 1, which consists of the condensate extraction pump (CEP), feedwater heaters with low pressure (FWHLP), feedwater heaters with high pressure (FWHHP), deaerator, feedwater pump (FWP), boiler, turbine, and the condenser. In the beginning, the pressure of the compressed liquid is increased by CEP, then its temperature is increased using FWHLP1, FWHLP2, and FWHLP3 which offer the heat transfer areas of 5.682, 4.219, and 3.321 m^2 respectively, to prepare the temperature and pressure conditions before introduction to the deaerator. The deaerator will remove oxygen and other dissolved gases from the liquids and pumpable compounds to prevent hazards to the boilers and turbines since the oxygen can cause the rapid corrosion of metal materials. The FWP and FWHHP1, FWHHP2, and FWHHP3, which have heat transfer areas of 17.112, 24.781, and 6.9 m^2

respectively, also increase the steam temperature and pressure before sending to the boilers to lighten the load of the reboilers for heating the steam to a high temperature of 600°C at which liquid steam will be converted to superheated vapor steam. The electric power can then be produced from the turbine with high pressure (HPT), and two turbines at intermediate pressure (IPT) and low pressure (LPT). Finally, the waste steam vapor from the last LPT will be sent to the condenser to condense the waste steam vapor into a compressed liquid as a cycle operation process. Information and thermodynamics details from [1] will be used as a base case in this work to determine the optimization and improvement through the alteration of the mass flow rate and operating temperature for each stream (each pressure steam condition is the same as proposed by [1]). The objective function in work includes thermal, exergy efficiency, and economy with multiple objectives.

B. Thermodynamic modelling and economic evaluation

The equations are used with a numerical process in order to solve to determine temperature and the enthalpy of the flow within the power plant. The following assumptions are made in line with similar investigations [27]:

- The definition of the thermodynamic reference status holds that P_0 = 1.01 bar while T_0 = 293.15 K
- All processes are examined under conditions of steady-state and steady-flow.
- The equipment used in the power plant is assumed to be working in adiabatic conditions.
- The fuel used was natural gas, while the lower heating value (LHV) = 46,515 kJ/kg [28]
- The power plant machinery was assumed to operate for 7,776 hours per year.
- The respective isentropic efficiencies for the pump, HPT, and LPT were 0.8, 0.85, and 0.9
- The effects of potential and kinetic energy were disregarded
- Annual revenue, labour costs, utility costs, ash handling and fuel storage costs, electrical or civil works, and the treatment costs for fumes are all ignored for this study
- The cost estimates (fixed and operating) cover a one-year period.

1) Energy analysis:

By balancing energy and mass, the system energy analysis can be performed through Equations (1) and (2), which allow the energy analysis of each of the system components to be made. In open systems under steady-state conditions, the first law of thermodynamics applies, and Table 1 presents the energy equations for each of the various components.

$$\sum_{in} \dot{m}_i = \sum_{out} \dot{m}_o \quad (1)$$

$$\sum \dot{Q}_i + \dot{m}\left(h_i + \frac{C_i^2}{2} + gZ_i\right) = \dot{m}\left(h_o + \frac{C_o^2}{2} + gZ_o\right) + \dot{W} \quad (2)$$

in which $\dot{Q}_i$ represents the transfer of heat from the source to the system at temperature T_i, while the network of the system is represented by W. The working fluid bulk velocity is given by C while Z shows the height above sea level of the stream and g indicates the specific force due to gravity.

2) Exergy analysis:

The second law of thermodynamics is employed to calculate exergy and to assess the system irreversibility. All of the procedures involved are irreversible. The exergy expression equations for each of the different streams are given as:

$$\dot{E}x_D = \sum_i \dot{m}_i ex_i - \sum_e \dot{m}_o ex_o + \dot{E}x_Q + \dot{E}x_W \quad (3)$$

$$\dot{E}x_Q = \left(1 - \frac{T_0}{T_i}\right)\dot{Q}_i \quad (4)$$

$$\dot{E}x_W = \dot{W} \tag{5}$$

in which $\dot{E}x_D$, $\dot{E}x_Q$ and $\dot{E}x_W$ represent exergy destruction, exergy rates arising due to the heat transfer and the work occurring over the control volume boundaries, respectively

Only the physical exergy associated with the mass flows across the control volume is taken into account and calculated using:

$$ex = ex_{ph} + ex_{ch} + ex_k + ex_{po} \tag{6}$$

There is no need to consider the kinetic (ex_k) and potential exergies (ex_{po}) [29].

Physical exergy (ex_{ph}) can be calculated from the following formula:

$$ex_{ph} = \dot{m}\left(h - h_0\right) + T_0\left(s - s_0\right) \tag{7}$$

Chemical exergy (ex_{ch}) from the gas mixtures is calculated on the basis of:

$$ex_{mix}^{ch} = \sum_{i=1}^{n} x_i ex_i^{ch} + RT_0 \sum_{i=1}^{n} x_i \ln x_i \tag{8}$$

The equation (8) given above is not suitable for the calculation of fuel exergy, and instead the simplified version given below can be applied:

$$ex_{ch} = ex_{fuel} = \lambda\left(LHV_{fuel}\right) \tag{9}$$

Where the situation involves a gaseous fuel, it is possible to employ the experimental formula C_xH_y, which was put forward by Dincer and Rosen [12] for calculations as:

$$\lambda = 1.033 + 0.0169\frac{y}{x} - \frac{0.0698}{x} \tag{10}$$

3) Economic analysis:

In performing the economic analysis for the power plant, the operating costs and the original capital investment are the key factors to be considered. The equipment costs include the acquisition of the steam turbine, boiler, and condenser, as well as the auxiliary items including the feedwater pumps, heater, condensate extraction pumps, and deaerator. The cost of this equipment is fixed and given as C_F , which can be expressed in terms of the component redundancies in each case [30]:

$$C_F = f\begin{pmatrix} C_{SB} + C_{ST} + C_C + n_{CEP}\left(C_{CEP}\right) \\ +n_{BFP}\left(C_{BFP}\right) + C_H + C_D \end{pmatrix} \tag{11}$$

In which reference value f is 1.87.

The original cost of each of the items or components represented by C_{Fi} was determined empirically from [4], [31] as shown:

- Steam turbine

$$C_{ST} = 633000\left(MWe\right)^{0.398} \tag{12}$$

- Condensate extraction pumps

$$C_{CEP} = 9000\left(MWe\right)^{0.4425} \tag{13}$$

- Steam boiler

$$C_{SB} = 1340000\left(MWe\right)^{0.694} \tag{14}$$

- Condenser

$$C_C = 398000\left(MWe\right)^{0.333} \tag{15}$$

Where MWe is the work rate produced in the steam power plant at the turbine.

- Boiler feed pumps

$$C_{BFP} = 35000\left(MWe\right)^{0.6107} \tag{16}$$

- Heater [32]

$$C_H = 6200(10.764A)^{0.42} \tag{17}$$

Where A is the heat-transfer area (m^2), which has the range of 1.858-185.806 m^2 [32]

- Deaerator [33]

$$C_D = 0.958M_{dea} + 30.0 \tag{18}$$

in which C_D represents the cost of the deaerator ($1000)(2002), and M_{dea} indicates the design water mass flow emanating from the deaerator in kg/s [34].

Overall operational costs will cover items such as insurance, maintenance, and fuel feedstock shown as [4], [31]:

$$C_O = \left(m_F C_F + C_M + C_I\right) \tag{19}$$

in which C_O represents the total operating cost, and F is fuel, M is maintenance, and I is insurance. In this instance. Maintenance is 3% of the total fixed cost, while insurance amounts to 2.5% [4], [31].

The equations determining the energy and destruction of exergy for each cycle component can be seen in Table 1. Exergy destruction is also known as irreversibility and is determined by the process of entropy generation. Entropy serves as an indication of the degree of randomness which exists within a particular system. In cases where less exergy is destroyed, and entropy generation is low, a system can be considered more orderly and offers the greater potential to work effectively. Furthermore, ambient temperatures also influence the rate of exergy destruction or irreversibility since it has a role to play in the equations which determine exergy destruction rates. Irreversibility increases as the ambient temperature rises.

III. OPTIMIZATION

A. Multi-objective optimization (MOO) of the formulation

The overall MOO problem can be expressed as shown [35]:

Minimize or maximize:

$$f(x) = \left[f_1(x), f_2(x), ..., f_k(x)\right]^T$$

Subject to: $g_j(x) \le 0; \quad j = 1, 2, ..., m$

in which k enumerates the objective functions while inequality constraints are enumerated by m.

This study makes use of a weighted sum technique in addressing the problem, which requires the use of predetermined scalar weights w_i allowing the minimization of the composite objective function shown as:

$$U = \frac{w_1}{f_1} + \frac{w_2}{f_2} + w_3 f_3 \tag{20}$$

in which U represents the minimum multi-objective desirability value.

This study makes use of three fitness functions. The first relates to energy efficiency as indicated by Equation (21); the second addresses exergy efficiency as indicated by Equation (22), while the third relates to the overall cost as indicated by Equation (23). These objectives have equal weightings, and therefore each weighting (w_k) can be allocated a value of 0.33 for equality of all three objective functions. These functions are expressed as follows:

Maximize energy efficiency:

$$f_1\left(T_i, m_i, h_i\right)_{i=1-28} = \frac{\dot{W}_T - \dot{W}_{CEP} - \dot{W}_{FWP}}{\dot{Q}_B} \tag{21}$$

Maximize exergy efficiency:

$$f_2\left(T_i, m_i, h_i, s_i\right)_{i=1-28} = \frac{\dot{W}_T - \dot{W}_{CEP} - \dot{W}_{FWP}}{ex_{fuel}} \tag{22}$$

Minimize overall cost:

$$f_3\left(T_i\right)_{i=1-28} = C_F + C_O \tag{23}$$

Subject to:

$25 \le T_1 \le 45.85$	$25 \le T_2 \le 50$	$40 \le T_3 \le 90$
$75 \le T_4 \le 110$	$100 \le T_5 \le 135$	$186 \le T_6 \le 187.92$
$194 \le T_7 \le 194.15$	$205 \le T_8 \le 237$	$270 \le T_9 \le 296$
$328 \le T_{10} \le 341$	$388 \le T_{12} \le 400$	$388 \le T_{12'} \le 400$
$73 \le T_{16} \le 74$	$475 \le T_{17} \le 485$	$318 \le T_{18} \le 321$
$318 \le T_{19} \le 321$	$285 \le T_{23} \le 304$	$205 \le T_{24} \le 245$

$195 \le T_{25} \le 203$ $80 \le T_{26} \le 116$ $44 \le T_{27} \le 94$
$30 \le T_{28} \le 55$ $33 \le T_{HW} \le 36$

B. SI algorithm

1) The sparrow search algorithm (SSA):

One interesting novel algorithm based on the concept of SI algorithm is the SSA [24], which was first developed in 2020 by Xue and Shen. The model is based on the foraging activities of flocks of sparrows as they look for food. The algorithm continually provides updates of the latest positions of the designated scroungers and producers as they conduct their search, and these updates are assessed to determine the optimal outcome through consideration of the fitness values.

The producer in the SSA generates foraging instructions for the whole sparrow population. The locations of discoverers are updated using a formula (24) which ensures that the algorithm cannot simply converge to the origin when attempting to optimize, and thus global optimization performance is improved. The following equation is used for the updates of the position of the producer:

$$X_{i,j}^{t+1} = \begin{cases} X_{i,j}^{t} \times (1+Q) & if \ \ R_2 < ST \\ X_{i,j}^{t} + (Q \times L) & if \ \ R_2 \ge ST \end{cases} \qquad (24)$$

In this form, the current number of iterations is given by t, while $iter_{\max}$ shows the maximum permissible number for those iterations. $X_{i,j}^{t}$ indicates the location details for the i^{th} sparrow positioned in the j^{th} dimension, while $\alpha \in (0,1]$ is simply a random number. The respective roles of $R_2 \left(R_2 \in [0,1]\right)$ and $ST \left(ST \in [0.5,1]\right)$ are to show the warning value and safety value. Q is a normally distributed random number while L is representative of a matrix which has a single element.

Table 1 Expression for energy efficiency, exergy efficiency, and exergy destruction rate and for double reheat steam power plant components

Equipment	Energy Balance Equations	Exergy Destruction Rate Equations	Exergy Efficiency
FWHLP1	$(\dot{m}_{10}-\dot{m}_{17}-\dot{m}_{12}-\dot{m}_{14}-\dot{m}_{19})(h_3-h_2)+(\dot{m}_{20}+\dot{m}_{21}+\dot{m}_{22})h_{28}-(\dot{m}_{20}+\dot{m}_{21})h_{27}-\dot{m}_7 h_{27}=0$	$\dot{I}_{FWHLP1}=-T_0[(\dot{m}_{10}-\dot{m}_{17}-\dot{m}_{12}-\dot{m}_{14}-\dot{m}_{19})(s_2-s_3)+(\dot{m}_{20}+\dot{m}_{21})s_{27}+\dot{m}_7 s_{22}-(\dot{m}_{20}+\dot{m}_{21}+\dot{m}_{22})s_{28}]$	$\eta_{\varepsilon,FWHLP1}=1-\frac{\dot{I}_{FWHLP1}}{\psi_{in,FWHLP1}}$
FWHLP2	$(\dot{m}_{10}-\dot{m}_{17}-\dot{m}_{12}-\dot{m}_{14}-\dot{m}_{19})(h_4-h_3)+(\dot{m}_{20}+\dot{m}_{21})h_{27}-\dot{m}_{20}h_{26}-\dot{m}_{21}h_{21}=0$	$\dot{I}_{FWHLP2}=-T_0[(\dot{m}_{10}-\dot{m}_{17}-\dot{m}_{12}-\dot{m}_{14}-\dot{m}_{19})(s_3-s_4)+\dot{m}_{20}s_{26}+\dot{m}_{21}s_{21}-(\dot{m}_{20}+\dot{m}_{21})s_{27}]$	$\eta_{\varepsilon,FWHLP2}=1-\frac{\dot{I}_{FWHLP2}}{\psi_{in,FWHLP2}}$
FWHLP3	$(\dot{m}_{10}-\dot{m}_{17}-\dot{m}_{12}-\dot{m}_{14}-\dot{m}_{19})(h_5-h_4)+(h_{26}-h_{20})\dot{m}_{20}=0$	$\dot{I}_{FWHLP3}=-T_0[(\dot{m}_{10}-\dot{m}_{17}-\dot{m}_{12}-\dot{m}_{14}-\dot{m}_{19})(s_4-s_5)+(s_{20}+s_{26})\dot{m}_{20}]$	$\eta_{\varepsilon,FWHLP3}=1-\frac{\dot{I}_{FWHLP3}}{\psi_{in,FWHLP3}}$
Deaerator	$\dot{m}_{19}h_{19}+(\dot{m}_{17}+\dot{m}_{12}+\dot{m}_{14})h_{25}+(\dot{m}_{10}-\dot{m}_{17}-\dot{m}_{12}-\dot{m}_{14}-\dot{m}_{19})h_5-\dot{m}_6 h_6=0$	$\dot{I}_{Deaerator}=-T_0[\dot{m}_{19}s_{19}+(\dot{m}_{17}+\dot{m}_{12}+\dot{m}_{14})s_{25}+(\dot{m}_{10}-\dot{m}_{17}-\dot{m}_{12}-\dot{m}_{14}-\dot{m}_{19})s_5-\dot{m}_6 s_6]$	$\eta_{\varepsilon,Deaerator}=1-\frac{\dot{I}_{Deaerator}}{\psi_{in,Deaerator}}$
FWHHP1	$\dot{m}_7 h_7-\dot{m}_8 h_8+\dot{m}_{14}h_{14}+(\dot{m}_{17}+\dot{m}_{12})h_{24}-(\dot{m}_{17}+\dot{m}_{12}+\dot{m}_{14})h_{25}=0$	$\dot{I}_{FWHHP1}=-T_0[\dot{m}_7 s_7+\dot{m}_{14}s_{14}+(\dot{m}_{17}+\dot{m}_{12})s_{24}-\dot{m}_8 s_8-(\dot{m}_{17}+\dot{m}_{12}+\dot{m}_{14})s_{25}]$	$\eta_{\varepsilon,FWHHP1}=1-\frac{\dot{I}_{FWHHP1}}{\psi_{in,FWHHP1}}$
FWHHP2	$\dot{m}_8 h_8-\dot{m}_9 h_9+\dot{m}_{17}h_{23}+\dot{m}_{12}h_{12}-(\dot{m}_{17}+\dot{m}_{12})h_{24}=0$	$\dot{I}_{FWHHP2}=-T_0[\dot{m}_8 s_8+\dot{m}_{17}s_{23}+\dot{m}_{12}s_{12}-\dot{m}_9 s_9-(\dot{m}_{17}+\dot{m}_{12})s_{24}]$	$\eta_{\varepsilon,FWHHP2}=1-\frac{\dot{I}_{FWHHP2}}{\psi_{in,FWHHP2}}$
FWHHP3	$\dot{m}_{10}h_{10}-\dot{m}_9 h_9-\dot{m}_{17}(h_{17}-h_{23})=0$	$\dot{I}_{FWHHP3}=-T_0[\dot{m}_9 s_9-\dot{m}_{10}s_{10}+\dot{m}_{17}(s_{17}-s_{23})]$	$\eta_{\varepsilon,FWHHP3}=1-\frac{\dot{I}_{FWHHP3}}{\psi_{in,FWHHP3}}$

Table 1 Expression for energy efficiency, exergy efficiency, and exergy destruction rate and for double reheat steam power plant components (cont.)

Equipment	Energy Balance Equations	Exergy Destruction Rate Equations	Exergy Efficiency
Condenser	$\dot{q}_C = (\dot{m}_{10} - \dot{m}_{17} - \dot{m}_{12} - \dot{m}_{14} - \dot{m}_{19} - \dot{m}_{20} - \dot{m}_{21} - \dot{m}_{22})h_{16} + (\dot{m}_{20} + \dot{m}_{21} + \dot{m}_{22})h_{28} - (\dot{m}_{10} - \dot{m}_{17} - \dot{m}_{12} - \dot{m}_{14} - \dot{m}_{19})h_1$	$\dot{I}_C = \{(\dot{m}_{10} - \dot{m}_{17} - \dot{m}_{12} - \dot{m}_{14} - \dot{m}_{19} - \dot{m}_{20} - \dot{m}_{21} - \dot{m}_{22})h_{16} + (\dot{m}_{20} + \dot{m}_{21} + \dot{m}_{22})h_{28} - (\dot{m}_{10} - \dot{m}_{17} - \dot{m}_{12} - \dot{m}_{14} - \dot{m}_{19})h_1\} - T_0\{(\dot{m}_{10} - \dot{m}_{17} - \dot{m}_{12} - \dot{m}_{14} - \dot{m}_{19} - \dot{m}_{20} - \dot{m}_{21} - \dot{m}_{22})s_{16} + (\dot{m}_{20} + \dot{m}_{21} + \dot{m}_{22})s_{28} - (\dot{m}_{10} - \dot{m}_{17} - \dot{m}_{12} - \dot{m}_{14} - \dot{m}_{19})s_1\} + \dot{m}_{w.in}\{(h_{w.in} - h_{w.out}) - T_0(s_{w.in} - s_{w.out})\}$	$\eta_{\varepsilon,C} = 1 - \frac{\dot{I}_C}{\psi_{in,C}}$
Boiler	$\dot{q}_B = \dot{m}_{11}h_{11} - \dot{m}_{10}h_{10} + (\dot{m}_{10} - \dot{m}_{17} - \dot{m}_{12})(h_{13} - h_{12'}) + (\dot{m}_{10} - \dot{m}_{17} - \dot{m}_{12} - \dot{m}_{14} - \dot{m}_{19})(h_{15} - h_{18})$	$\dot{I}_B = \{\dot{m}_{10}(h_{10} - h_{11}) + (\dot{m}_{10} - \dot{m}_{17} - \dot{m}_{12})(h_{12'} - h_{13}) + (\dot{m}_{10} - \dot{m}_{17} - \dot{m}_{12} - \dot{m}_{14} - \dot{m}_{19})(h_{18} - h_{15}) - T_0[(s_{10} - s_{11}) + (\dot{m}_{10} - \dot{m}_{17} - \dot{m}_{12})(s_{12'} - s_{13}) + (\dot{m}_{10} - \dot{m}_{17} - \dot{m}_{12} - \dot{m}_{14} - \dot{m}_{19})(s_{18} - s_{15})]\} + \dot{q}_B(1 - \frac{T_0}{T_B})$	$\eta_{\varepsilon,B} = 1 - \frac{\dot{I}_B}{ex_{fuel}}$
FWP	$\dot{W}_{FWP} = \dot{m}_7(h_7 - h_6)$	$\dot{W}_{FWP} = \dot{m}_7[(h_6 - h_7) - T_0(s_6 - s_7)] + \lvert\dot{W}_{FWP}\rvert$	$\eta_{\varepsilon,FWP} = 1 - \frac{\dot{I}_{FWP}}{\dot{W}_{FWP}}$
CEP	$\dot{W}_{CEP} = (\dot{m}_{10} - \dot{m}_{17} - \dot{m}_{12} - \dot{m}_{14} - \dot{m}_{19}) \times (h_2 - h_1)$	$\dot{I}_{CEP} = (\dot{m}_{10} - \dot{m}_{17} - \dot{m}_{12} - \dot{m}_{14} - \dot{m}_{19})[(h_1 - h_2) - T_0(s_1 - s_2)] + \lvert\dot{W}_{CEP}\rvert$	$\eta_{\varepsilon,CEP} = 1 - \frac{\dot{I}_{CEP}}{\dot{W}_{CEP}}$
Turbine	$\dot{W}_t = \{\dot{m}_{11}(h_{11} - h_{17}) + (\dot{m}_{10} - \dot{m}_{17})(h_{17} - h_{12}) + (\dot{m}_{10} - \dot{m}_{17} - \dot{m}_{12})(h_{13} - h_{14}) + (\dot{m}_{10} - \dot{m}_{17} - \dot{m}_{12} - \dot{m}_{14})(h_{14} - h_{18}) + (\dot{m}_{10} - \dot{m}_{17} - \dot{m}_{12} - \dot{m}_{14} - \dot{m}_{19}) \times (h_{15} - h_{20}) + (\dot{m}_{10} - \dot{m}_{17} - \dot{m}_{12} - \dot{m}_{14} - \dot{m}_{19} - \dot{m}_{20}) \times (h_{20} - h_{21}) + (\dot{m}_{10} - \dot{m}_{17} - \dot{m}_{12} - \dot{m}_{14} - \dot{m}_{19} - \dot{m}_{20} - \dot{m}_{21})(h_{21} - h_{22}) + (\dot{m}_{10} - \dot{m}_{17} - \dot{m}_{12} - \dot{m}_{14} - \dot{m}_{19} - \dot{m}_{20} - \dot{m}_{21} - \dot{m}_{22})(h_{22} - h_{16})\}$	$\dot{I}_t = \{-T_0[\dot{m}_{11}(s_{11} - s_{17}) + (\dot{m}_{10} - \dot{m}_{17})(s_{17} - s_{12}) + (\dot{m}_{10} - \dot{m}_{17} - \dot{m}_{12})(s_{13} - s_{14}) + (\dot{m}_{10} - \dot{m}_{17} - \dot{m}_{12} - \dot{m}_{14})(s_{14} - s_{18}) + (\dot{m}_{10} - \dot{m}_{17} - \dot{m}_{12} - \dot{m}_{14} - \dot{m}_{19}) \times (s_{15} - s_{20}) + (\dot{m}_{10} - \dot{m}_{17} - \dot{m}_{12} - \dot{m}_{14} - \dot{m}_{19} - \dot{m}_{20}) \times (s_{20} - s_{21}) + (\dot{m}_{10} - \dot{m}_{17} - \dot{m}_{12} - \dot{m}_{14} - \dot{m}_{19} - \dot{m}_{20} - \dot{m}_{21})(s_{21} - s_{22}) + (\dot{m}_{10} - \dot{m}_{17} - \dot{m}_{12} - \dot{m}_{14} - \dot{m}_{19} - \dot{m}_{20} - \dot{m}_{21} - \dot{m}_{22})(s_{22} - s_{16})\}$	$\eta_{\varepsilon,t} = 1 - \frac{\dot{W}_t}{\dot{W}_t + \dot{I}_t}$

The scrounger locations are then updated as shown:

$$X_{i,j}^{t+1} = \begin{cases} Q \times \exp\left(\dfrac{X_{worst}^t - X_{i,j}^t}{i^2}\right) & if\ i < \dfrac{n}{2} \\ X_P^{t+1} + \left|X_{i,j}^{t+1} - X_P^{t+1}\right| \times A^+ \times L & otherwise \end{cases} \tag{25}$$

This formula X_P represents the best location reached by the current producer while X_{worst} indicates the worst location currently occupied globally. A represents a matrix of $1 \times d$ in which the elements are each given a random value of either 1 or -1, so that $A^+ = A^T\left(AA^T\right)^{-1}$

$$X_{i,j}^{t+1} = \begin{cases} X_{best}^t + \beta \times \left|X_{i,j}^t - X_{best}^t\right| & if\ f_i > f_g \\ X_{i,j}^t + K \times \left(\dfrac{\left|X_{i,j}^t - X_{worst}^t\right|}{(f_i - f_w) + \varepsilon}\right) & if\ f_i = f_g \end{cases} \tag{26}$$

In this case, the current global optimum is given by X_{best} while β serves as a parameter of step-length control with a normal distribution of mean 0 and variance 1. The direction taken by each sparrow is given by K while f_i is the fitness value for the current sparrow and f_g indicates the best current fitness value while f_w is the worst current fitness value. Finally, ε indicates the smallest constant.

Algorithm 1 The framework of the SSA [24]

Input:

Initialize a population of n sparrows and define its relevant parameters including G (the maximum iterations), PD (the number of producers), SD (the number of sparrows n),

Output: x_{best}, f_g .

1. while ($t < G$)
2. Place the fitness values in order, identifying the current best and current worst items;
3. $R_2 = rand(1)$
4. **for** $i = 1 : PD$
5. Update the location of the sparrow via Equation (24);
6. **end for**
7. **for** $i = (PD+1) : n$
8. Update the location of the sparrow via Equation (25);

Algorithm 1 The framework of the SSA [24] (cont.)

9. **end for**
10. **for** $i = 1:SD$
11. Update the location of the sparrow via Equation (26);
12. end for
13. Obtain the latest current location;
14. In the event that this new location is superior to the previous location, it should be updated;
15. t = t+1
16. end while
17. return x_{best}, f_g

2) The artificial jellyfish search (JS) optimizer:

Another example among the latest meta-heuristic SI algorithm approaches is the JS, which is based on the behavioural tendencies of jellyfish. It was created by Chou and Truong in 2020. To simulate the behavior of jellyfish swarms in the ocean, it is necessary to model the activity of each jellyfish and the sea current at any given moment, along with implementing a means of control for the timing of the actions. JS achieves optimized convergence through balancing the activities of exploration and utilization within the search area. In the open ocean, jellyfish move to search for food, and therefore they are inclined to move constantly towards areas rich in food. A more detailed explanation of the workings of the JS optimizer can be found in [25].

3) Cooperation search algorithm (CSA):

In 2020, Feng et al. created a novel algorithm known as CSA, and it is based on the nature of collaborative activity in modern organizations. Initially, a random set of potential solutions is generated within the search space before three operators are allowed to run until the predetermined stopping criterion is reached. The first operator is the team communication operator in which the list headed Algorithm 1 presents the details of the procedure for implementing CSA enhances global exploration and serves to identify the search area with the greatest potential. Second is the reflective learning operator which serves to balance the exploration and exploitation activities. Finally, the internal competition operator selects solutions which offer the greatest potential for subsequent cycles. More details concerning the CSA can be found in [26].

IV. RESULTS AND DISCUSSION

The 3E analysis for the steam power plant based on energy efficiency, exergy efficiency, and economic evaluation is calculated and optimized using the parameters of temperature, pressure, enthalpy, and entropy via thermodynamic and economic modelling using MATLAB software R2021a (Master License: 31557780). The balance of mass and energy, and exergy can be determined for all of the plant equipment, while the decision variable of the calculations is the temperature of each of the streams.

The running performance can be assessed by running the test 30 times using each algorithm under the same fitness conditions governing the initial iteration in the case of each of the three algorithms, including SSA, JS, and CSA methods. The set up was arranged such that the population size was 50 and the maximum iterations amounted to 500. The MATLAB software was then used to run the optimizations using the SSA, JS, and CSA methods. The solutions are presented in terms of the multi-objective desirability value (U), which is summarized in Table 2 based on the statistical data for the different algorithms.

In conclusion, SSA was found to offer the best performance in searching for solutions and determining global (or near-global) optima and therefore achieved the leading multi-objective desirability value (U). The robustness of SSA was also superior to JS and CSA methods as evidenced from the standard deviation (SD.). In terms of central processing unit time (CPU. Time), the three algorithms produced broadly similar results.

The best solution performance from the 30 runs was selected for each of the three algorithms, and the association between the multi-objective desirability value (U) and the number of iterations was determined in order to assess the convergence rate for the solution, as can be seen in Figure 2. For the best solutions of SSA, JS, and CSA methods, the number of iterations amounted to 261, 299, and 157, respectively. Although CSA had a significantly faster convergence rate, its optimal results were not satisfactory, at 2,060,496, while SSA achieved a superior outcome of 2,037,752 and JS was also better at 2,057,431.

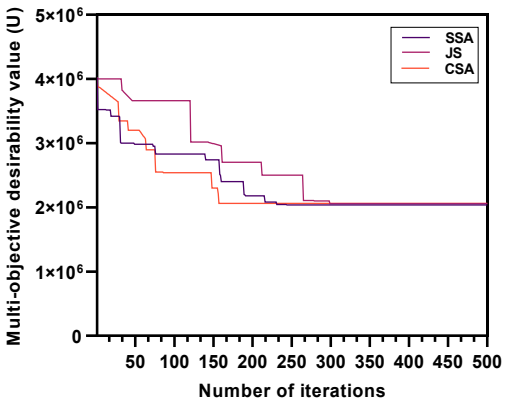

Figure 2 Convergence rate characteristics of multi-objective desirability value (U) for the three different algorithms.

Table 2 Statistical results in the double reheat steam power plant using the three different algorithms

SI algorithm	SSA	JS	CSA
Mean	2,042,636	2,063,922	2,065,366
Best	2,037,752	2,057,431	2,060,496
Worst	2,064,751	2,087,596	2,086,261
SD.	8,157.266	11,180.78	9,177.15
CPU. average time	65.48 s	63.57 s	66.41 s

For the optimal values reported, the decision variables from the MATLAB software and the test results from the SSA, JS, and CSA methods and from [1] can be seen in Table 3. In Table 3 the temperature and mass flow rate values of each of the streams prior to optimization are presented [1], and the same parameter values are shown following optimization via SSA, JS, and CSA methods. The thermodynamic operational properties for the different streams in the steam are shown in Table 4 under SSA.

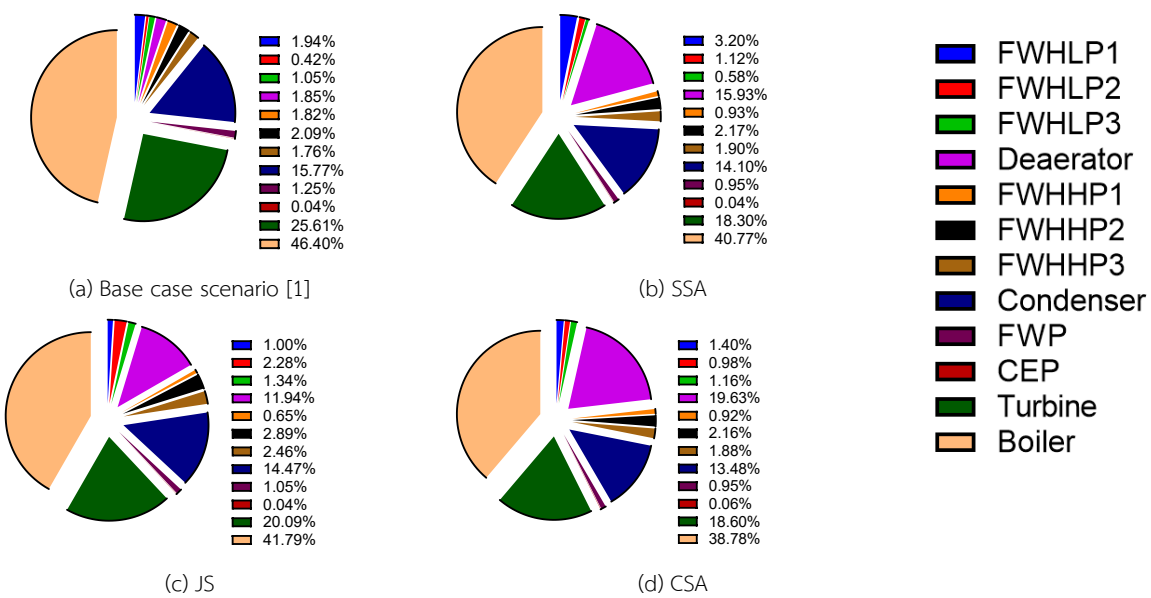

(a) Base case scenario [1]

(b) SSA

(c) JS

(d) CSA

Figure 3 The destruction of exergy in steam power plants with double reheat

Table 5 indicates that the power balance based on the steam power plant with double reheat for the three algorithms SSA, JS, and CSA methods, has a higher duty at the boiler and the condenser than reported by [1]. This is because the inlet temperature at the boiler (stream 10) of all three algorithms obtained from calculations using the MATLAB tool is lower than the values obtained by [1] (shown in Table 3.), resulting in higher energy requirements for heating the temperature steam to 600°C. In addition, it can be observed that the three algorithms also have the higher condenser duty than traditional work due to their large differences in temperature output (stream 1) and input (stream 16) of the condenser is greater than for traditional work, resulting in a greater energy requirement for cooling the steam down. Accordingly, this increases the utility cost since a more incredible amount of energy is necessary. However, when considering the steam turbine, which has the role of obtaining heat energy from the pressurized steam before converting it to mechanical work, three algorithms can promote the energy produced from [1], which amounts to only 1,311.5 kW due to the greater mass flow rate of the three algorithms at the inlet (stream 15) of the LP turbine which is the main component in producing energy. The turbine power output can be expressed in the form of the mass flow rate of the working substance and the enthalpy drop, which appears as $P_{op} = m_w \Delta h$, in which $\Delta h = h_{in} - h_{out}$.

Exergy destruction in the steam power plant with double reheat shown in Figure 3 demonstrates that within the power plant, the boiler, turbine, condenser, and deaerator are sources of exergy destruction as shown in the percentage fraction pie chart. The greatest exergy destruction of the based case and all algorithms were due to the boiler since the boiler system is the main destroyer of exergy from high-temperature operations [36]. Since this work set the ambient temperature at 25°C while the boiler is operated at 600°C, the lower ambient temperature can cause an increase in the irreversibility rate of the boiler. It is noteworthy that there is no need to consider the reference environment state when performing the calculations for any alteration in a thermodynamic property (analysis of the first law), although it does influence exergy (analysis of the second law).

Table 3 The decision variables for each of the streams prior to and following optimization

Stream	Before Optimization			After Optimization each algorithm					
	Base case scenario [1]			SSA		JS		CSA	
	$\dot{m}$ (kg/s)	T (°C)	Phase	$\dot{m}$ (kg/s)	T (°C)	$\dot{m}$ (kg/s)	T (°C)	$\dot{m}$ (kg/s)	T (°C)
1	0.6416	45.79	C	0.6532	27.67	0.647	29.26	0.6612	34.75
2	0.6416	45.9	C	0.6532	27.77	0.647	29.37	0.6612	34.91
3	0.6416	85.99	C	0.6532	77.73	0.647	43.91	0.6612	63.12
4	0.6416	107.6	C	0.6532	101.01	0.647	79.55	0.6612	83.87
5	0.6416	134.6	C	0.6532	114.56	0.647	100.61	0.6612	104.78
6	1	187.9	C	0.97	187.92	0.9935	187.92	0.9817	187.92
7	1	194.1	C	0.97	194.05	0.9935	194.05	0.9817	194.05
8	1	236.8	C	0.97	217.42	0.9935	205.88	0.9817	217.42
9	1	295.7	C	0.97	281.30	0.9935	272.13	0.9817	281.40
10	1	340.8	C	0.97	336.23	0.9935	329.76	0.9817	336.25

Table 3 The decision variables for each of the streams prior to and following optimization (cont.)

Stream	Before Optimization			After Optimization each algorithm					
	Base case scenario [1]			SSA		JS		CSA	
	$\dot{m}$ (kg/s)	T (°C)	Phase	$\dot{m}$ (kg/s)	T (°C)	$\dot{m}$ (kg/s)	T (°C)	$\dot{m}$ (kg/s)	T (°C)
11	1	600	V	0.97	600.00	0.9935	600.00	0.9817	600.00
12	0.1165	395.5	V	0.1067	389.43	0.1093	389.43	0.108	389.43
12'	0.7545	395.5	V	0.7178	389.43	0.7352	389.43	0.7265	389.43
13	0.7545	600	V	0.7178	600.00	0.7352	600.00	0.7265	600.00
14	0.05638	452.2	V	0.0287	452.23	0.0147	452.23	0.0291	452.23
15	0.6416	600	V	0.6532	600.00	0.647	600.00	0.6611	600.00
16	0.5575	73.35	V	0.5552	73.49	0.5823	73.49	0.595	73.49
17	0.1289	483.3	V	0.1455	476.73	0.149	476.73	0.1473	476.73
18	0.6416	320.1	V	0.6532	319.97	0.647	319.97	0.6611	319.97
19	0.05653	320.1	V	0.0359	319.97	0.0735	319.97	0.0363	319.97
20	0.0262	406.6	V	0.0131	406.57	0.0194	406.57	0.0198	406.57
21	0.002087	303.7	V	0.0588	303.68	0.0323	303.68	0.0198	303.68
22	0.037	222.5	V	0.0261	222.43	0.0129	222.43	0.0264	222.43
23	0.1289	303.7	C	0.1455	295.67	0.149	286.93	0.1473	296.24
24	0.2455	244.8	C	0.2522	218.42	0.2583	206.88	0.2553	218.42
25	0.3019	202.1	C	0.2809	195.05	0.273	195.05	0.2843	195.05
26	0.0262	115.6	C	0.0131	102.01	0.0194	80.55	0.0198	84.87
27	0.04707	93.99	C	0.0719	109.63	0.0518	44.91	0.0397	64.12
28	0.08407	53.9	C	0.098	87.99	0.0647	30.37	0.0661	35.91
Cold water	32.65	25	C	40	25.00	40	25.00	40	25.00
Hot water	32.65	35	C	40	33.68	40	33.76	40	33.87

Where V represent superheated vapor steam and C represent the compressed liquid steam

Table 4 Thermodynamic properties of the double reheat steam power plant obtained using SSA for each of the streams

Stream	$\dot{m}$ (kg/s)	P (kPa)	T (°C)	Phase	h (kJ/kg)	s (kJ/kg.K)	Ψ (kJ/kg.K)
1	0.6532	10	27.67	C	116.01	0.404	0.136
2	0.6532	1,199	27.77	C	117.519	0.406	0.732
3	0.6532	1,199	77.73	C	326.349	1.048	12.109
4	0.6532	1,199	101.01	C	424.181	1.318	23.43
5	0.6532	1,199	114.56	C	481.426	1.468	31.61
6	0.97	1,199	187.92	C	798.3	2.216	137.983
7	0.97	30,000	194.05	C	839.289	2.234	172.536
8	0.97	30,000	217.42	C	941.563	2.448	209.852
9	0.97	30,000	281.30	C	1,235.865	3.011	332.502
10	0.97	30,000	336.23	C	1,524.784	3.507	469.308
11	0.97	30,000	600.00	V	3,446.872	6.237	1,544.202

Table 4 Thermodynamic properties of the double reheat steam power plant obtained using SSA for each of the streams (cont.)

Stream	$\dot{m}$ (kg/s)	P (kPa)	T (°C)	Phase	h (kJ/kg)	s (kJ/kg.K)	Ψ (kJ/kg.K)
12	0.1067	8,307	389.43	V	3,102.6	6.295	131.283
12'	0.7178	8,307	389.43	V	3,102.6	6.295	883.179
13	0.7178	8,307	600.00	V	3,639.894	7.002	1,117.541
14	0.0287	3,277	452.23	V	3,345.954	7.048	35.853
15	0.6532	1,199	600.00	V	3,696.998	7.946	870.421
16	0.5552	10	73.49	V	2,636.925	8.308	91.356
17	0.1455	15,121	476.73	V	3,240.031	6.252	200.884
18	0.6532	1,199	319.97	V	3,089.638	7.108	636.895
19	0.0359	1,199	319.97	V	3,089.638	7.108	35.004
20	0.0131	327.7	406.57	V	3,288.695	8.014	11.842
21	0.0588	141.6	303.68	V	3,080.948	8.068	39.991
22	0.0261	65	222.43	V	2,921.195	8.128	13.115
23	0.1455	15,121	295.67	C	1,314.489	3.186	53.724
24	0.2522	8,307	218.42	C	938.149	2.492	50.392
25	0.2809	3,277	195.05	C	830.956	2.281	43.687
26	0.0131	3,277	102.01	C	429.949	1.327	0.51
27	0.0719	141.6	109.63	V	2,690.505	7.242	38.535
28	0.098	65	87.99	C	368.514	1.169	2.413
Cold water	40	101	25.00	C	104.929	0.367	6.345
Hot water	40	101	33.68	C	141.214	0.487	26.625

Where V represent superheated vapor and C represent the compressed liquid

Table 5 The power of main equipment in the double reheat steam power plant process

Equipment	Base case scenario [1]	SSA	JS	CSA
Boiler (kW)	2,581	2,646.382	2,734.23	2,678.32
Condenser (kW)	1,312	1,450.872	1,464.258	1,482.46
Turbine (kW)	1,311.5	1,351.66	1,377.247	1,381.27
Feed water pump (kW)	41.18	39.76	40.72	40.24
Condense extraction pump (kW)	1.7	0.993	0.9963	1.17

Therefore, these conditions should enhance the performance of the boiler and bring about a significant rise in the efficiency of the plant. This issue can be reduced by preheating the steam before sending it to the boiler [37]. In the case of exergy being destroyed within the system's heat exchangers, such as the condenser or the feedwater heater, this occurs because of the substantial difference in temperature between hot fluids and cold fluids. The three algorithms achieve slightly lower exergy destruction than in the base case scenario [1], and this suggests that the rate of irreversibility for the turbine is lower than was the case in the study conducted by [1].

The fixed cost in this paper was calculated from the equipment purchase cost (Eqs. 11-18) and also the operating cost which is calculated from maintenance,

insurance, and purchase of fuel feedstock (Eq. 19) and can be seen in Figure 4 (a).

The comparison of the operating cost of the three algorithms in Figure 4 (b) indicates that the highest fixed cost and operating cost is for the CSA, because of the high duty energy consumption of the boiler and the condenser shown respectively in Table 5 as 2,678.32 kW and 1,482.46 kW. Additionally, the highest 1,381.27 kW energy produced from the CSA turbine significantly increases the fixed cost due to the energy produced being a function of the fixed cost Equations 11-18 for many items of equipment. The power balance in the turbine is 1,377.247 kW and 1,351.66 kW of energy produced for the JS and SSA methods, respectively, which are less than for the CSA. In contrast, SSA has the lowest fixed cost including the operating cost when compared with JS and CSA. That means that SSA used the lowest amount of fuel, and also had the lowest fixed cost which can result in the lowest operating cost due to the fixed cost being a function of the operational cost. In the meantime, SSA can still maintain the efficiency of energy produced when compared with JS that has a higher fixed cost and operating cost. These hints can imply that SSA is an appropriate choice for this steam power plant when considering the economic aspect.

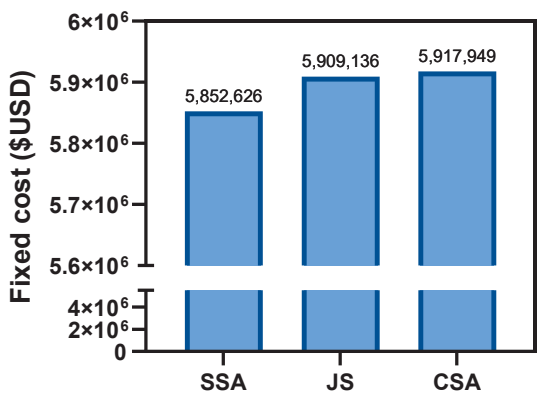

(a)

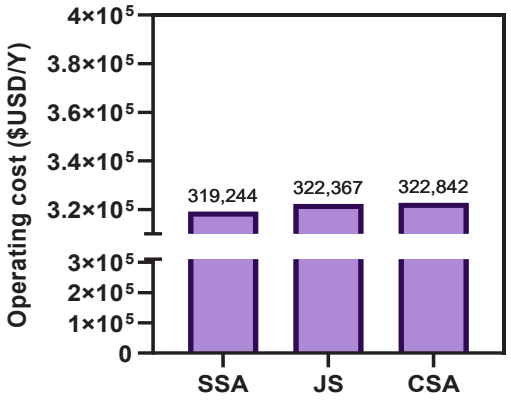

(b)

Figure 4 Steam power plant economic evaluation using double reheat (a) Fixed cost ($USD), (b) Operating cost ($USD/yr)

Table 6 indicates that the three algorithms have a higher enthalpy efficiency and exergy efficiency than in the base case except for the enthalpy efficiency of JS which is slightly lower than [1] by 0.06%. This means the three algorithms can wisely use the amount of heated steam at constant pressure for heat transferring in the six heat exchangers in a manner that improved upon the pre-optimization conditions. In addition, the three algorithms can show that this steam power plant optimized the maximum level of useful work obtained within a given process in which the system obtains a dead state. Thus, one may infer that the three algorithms successfully improve both the enthalpy efficiency and the exergy efficiency from the work of [1].

After the three algorithms' optimization results revealed that the CSA has the highest enthalpy efficiency and exergy efficiency at 50.03% and 48.53% respectively, the reduced level of exergy destruction seen in Figure 3 is likely to offer a substantial advantage in terms of exergy efficiency. It is possible to define this exergy efficiency in terms of only physical exergy while ignoring kinetic and potential exergy components since their lack of size renders them insignificant. It is possible

to offer the description of physical exergy as the maximum theoretically feasible extent of useful work that a system might accomplish during its interaction with an equilibrium state. Significantly, the overall performance should have its basis in efficiency as defined by the second law of thermodynamics, which can be applied to describe exergy efficiency, whereas the first law is only concerned with energy efficiency [36]. Consequently, the JS has the lowest efficiency compared with the other two algorithms, but it still offers better exergy efficiency than in the work of base case scenario [1]. However, the SSA is most valuable when considering the economic cost because the SSA has enthalpy efficiency slightly different from the CSA by 0.49%. In the meantime, the exergy efficiency difference between SSA and CSA is 0.47%. Thus, the SSA method can achieve cost savings of up to $USD 68,921. According to the multi-objective desirability value (U) of SSA, which was the lowest value in comparison with JS and CSA, it makes sense that we can choose SSA as the best algorithm among the three for the reasons mentioned in order to achieve steam power plant improvement.

Table 6 3E analysis resulted from the different optimization algorithm

3E analysis	Base case scenario [1]	SSA	JS	CSA
Enthalpy efficiency	48.90%	49.54%	48.84%	50.03%
Exergy efficiency	46.13%	48.06%	47.38%	48.53%
Economic cost ($USD)	-	6,175,006	6,234,639	6,243,927
Multi-objective desirability value (U)		2,037,752	2,057,431	2,060,496

V. CONCLUSION

An analysis was carried out to examine the 3E aspects of a steam power plant which used double reheat and feedwater heaters. The energy, exergy, and economic factors were addressed using multi-objective optimization via SI algorithm including SSA, JS, and CSA methods. When comparing the results with those of [1], which is defined as a base case in this work, it was found that the optimal results were achieved using SSA method in terms of search performance and the achievement of global optima. Accordingly, SSA method achieved a fitness of 2,037,752, which represented the best multi-objective desirability value (U) obtained from a trial set of 30 runs. The SSA method also offered superior robustness compared to JS and CSA methods, taking the SD. values as evidence. The three algorithms showed little difference when their CPU. times were evaluated, while none of the three algorithms could successfully solve the issue of exergy destruction at the boiler, although it is well known that the boiler is the main site where exergy destruction takes place when the system is operated at high temperatures. However, all three algorithms were able to support the energy production of turbine power with SSA, JS, and CSA methods achieving 1,351.66 kW, 1,377.247 kW, and 1,381.27 kW respectively, which compares favorably with the base case which reported 1,311.5 kW. One further advantage of the three algorithms is that all three were able to make effective use of the heated steam at constant pressure when performing transfers among the six heat exchangers, since enthalpy and exergy efficiencies were increased significantly by the algorithms. The sole exception came in the case of JS, for which the enthalpy efficiency was the lowest among those algorithms. From the economic perspective, SSA delivered reduced costs by up to $USD 68,921. Finally, SSA's multi-objective desirability value (U) was the lowest among

the three algorithms, leading to the conclusion that SSA method would be more appropriate than JS or CSA methods. From these findings, it is possible to conclude that 3E analysis can be effectively performed using a SI algorithms technique. It was found that multi-objective optimization analysis could be employed to further improve upon the result from previous study [1].

REFERENCES

[1] M. M. Rashidi, A. Aghagoli, and M. Ali, "Thermodynamic analysis of a steam power plant with double reheat and feed water heaters," *Advances in Mechanical Engineering*, vol. 6, pp. 1–11, Mar. 2014.

[2] S. Elahifar, E. Assareh, and R. Moltames, "Exergy analysis and thermodynamic optimisation of a steam power plant-based Rankine cycle system using intelligent optimisation algorithms," *Australian Journal of Mechanical Engineering*, pp. 1–12, Sep, 2019.

[3] C. D. Weir, "Optimization of heater enthalpy rises in feed-heating trains," *Institution of Mechanical Engineers*, *vol. 174*, no. 1, pp. 769–796, Jun. 1960.

[4] P. G. Potter, *Power plant theory and design*, New York, NY, USA: Krieger Publishing Company, 1989.

[5] S. Farhad, M. S. Avval, and M. Y. Sinaki, "Efficient design of feedwater heaters network in steam power plants using pinch technology and exergy analysis," *Int. Journal of Energy Research*, vol. 32, no. 1, pp. 1–11, Jan. 2008.

[6] S. N. Naserabad, A. Mehrpanahi, and G. Ahmadi, "Multi-objective optimization of feed-water heater arrangement options in a steam power plant repowering," *Journal of Cleaner Production*, vol. 220, pp. 253–270, May. 2019.

[7] S. Khanmohammadi, A. R. Azimian, and S. Khanmohammadi, "Exergy and exergoeconomic evaluation of Isfahan steam power plant," *Int. Journal of Exergy*, vol. 12, no. 2, pp. 249–272, Jan. 2013.

[8] A. Bejan, G. Tsatsaronis, and M. Moran, *Thermal design and optimization*, New York, NY, USA: Wiley, 1996.

[9] R. Kumar, "A critical review on energy, exergy, exergoeconomic and economic (4-E) analysis of thermal power plants," *Engineering Science and Technology, an Int. Journal*, vol. 20, no. 1, pp. 283–292, Feb. 2017.

[10] G. Ahmadi, D. Toghraie, and O. Akbari, "Energy, exergy and environmental (3E) analysis of the existing CHP system in a petrochemical plant," *Renewable and Sustainable Energy Reviews*, vol. 99, pp. 234–242, Jan. 2019.

[11] I. Lee, K. Tak, H. Kwon, J. Kim, and I. Moon, "Design and optimization of a pure refrigerant cycle for natural gas liquefaction with subcooling," *Industrial & Engineering Chemistry Research*, vol. 53, no. 25, pp. 10397–10403, Jun. 2014.

[12] M. A. Rosen and I. Dincer, "Exergo-economic analysis of power plants operating on various Fuels," *Applied Thermal Engineering*, vol. 23 no. 6, pp. 643–658, Apr. 2003.

[13] S. O. Oyedepo, O. Kilankso, M. A. Waheed, O .S. Fayomi, O. S. Ohunakin, P. O. Babalola, S. O. Ongbali, C. N. Nwaokocha, B. Mabinuori, and O. O. Shopeju, "Dataset on thermodynamics performance analysis and optimization of a reheat–regenerative steam turbine power plant with feed water heaters," *Data in Brief*, vol. 32, pp. 1–7, Oct. 2020.

[14] S. E. K. Fateen and A. B. Petriciolet, "On the effectiveness of nature-inspired metaheuristic algorithms for performing phase equilibrium thermodynamic calculations," *The Scientific World Journal*, vol. 2014, pp. 1–12, Aug. 2014.

[15] M. M. Keshtkar, "Effect of subcooling and superheating on performance of a cascade refrigeration system with considering thermo-economic analysis and multi-objective optimization," *Journal of Advanced Computer Science & Technology*, vol. 5, no. 2, pp. 42–47, 2016.

[16] H. Sayyaadi, E. H. Amlashi, and M. Amidpour, "Multi-objective optimization of a vertical ground source heat pump using evolutionary algorithm," *Energy Conversion and Management,* vol. 50, no. 8, pp. 2035–2046, Aug. 2009.

[17] M. M. Keshtkar and P. Talebizadeh, "Multi-objective optimization of cooling water package based on 3E analysis: A case study," *Energy*, vol. 134, pp. 840–849, Sep. 2017.

[18] M. R. Kolahi, M. Amidpour, and M. Yari, "Multi-Multi-objective metaheuristic optimization of combined flash-binary geothermal and humidification dehumidification desalination systems," *Desalination*, vol. 490, pp. 1–12, Sep. 2020.

[19] R. Dufo-Lopez, J. L. Bernal-Agustin, and J. Contreras, "Optimization of control strategies for stand-alone renewable energy systems with hydrogen storage," *Renewable Energy*, vol. 32, no.7, pp. 1102–1126, Jun. 2007.

[20] A. M. Abdelshafy, H. Hassan, and J. Jurasz, "Optimal design of a grid-connected desalination plant powered by renewable energy resources using a hybrid PSO–GWO approach," *Energy Conversion and Management*, vol. 173, pp. 331–347, Oct. 2018.

[21] M. Mavrovouniotis, C. Li, and S. Yang, "A survey of swarm intelligence for dynamic optimization: Algorithms and applications," *Swarm and Evolutionary Computation*, vol. 33, pp. 1–7, Apr. 2017.

[22] A. Colorni, M. Dorigo, and V. Maniezzo, "Distributed optimization by ant colonies," in *Proc. the First European Conf. Artificial Life*, Paris, France, Dec. 11-13, 1991, pp. 134–142.

[23] J. Kennedy and R. Eberhart, "Particle swarm optimization," in *Proc. the IEEE Int. Conf. Neural Networks*, Perth, Australia, Nov. 27, 1995, pp. 1942–1948.

[24] J. Xue and B. Shen, "A novel swarm intelligence optimization approach: sparrow search algorithm," *Systems Science & Control Engineering*, vol. 8, no. 1, pp. 22–34, Jan. 2020.

[25] J. S. Chou and D. N. Truong, "A novel metaheuristic optimizer inspired by behavior of jellyfish in ocean," *Applied Mathematics and Computation*, vol. 389, pp. 1–47, Jan. 2021.

[26] Z. K. Feng, W. J. Niu, and S. Liu, "Cooperation search algorithm: A novel metaheuristic evolutionary intelligence algorithm for numerical optimization and engineering optimization problems," *Applied Soft Computing*, vol. 98, pp. 1–27, Jan. 2021.

[27] M. H. Ahmadi, M. A. Nazari, M. Sadeghzadeh, F. Pourfayaz, M. Ghazvini, T. Ming, J. P. Meyer, and M. Sharifpur, "Thermodynamic and economic analysis of performance evaluation of all the thermal power plants: A review," *Energy Science & Engineering*, vol. 7, no. 1, pp. 30–65, Feb. 2019.

[28] H. Kurt, Z. Recebli, and E. Gedik, "Performance analysis of open cycle gas turbines," *Int. Journal of Energy Research*, vol. 33, no. 3, pp. 285–294, Mar. 2009.

[29] Y. A. Cengel, and M. A. Boles, T*hermodynamics: An engineering aproach*, 6th ed. New York, NY, USA: The McGraw-Hill Companies, 2007.

[30] R. Kumar, A. K. Sharma, and P. C. Tewari, "Thermal performance and economic analysis of 210 MWe coal-fired power plant," *Journal of Thermodynaics*, vol. 2014, pp. 1–10, Feb. 2014.

[31] A. C. Caputo, M. Palumbo, P. M. Pelagagge, and F. Scacchia, "Economics of biomass energy utilization in combustion and gasification plants: effects of logistic variables," *Biomass and Bioenergy*, vol. 28, no. 1, pp. 35–51, Jan. 2005.

[32] W. D. Seider, J. D. Seader, D. R. Lewin, and S. Widagdo, *Product and process design principles*, 3rd ed. Hoboken, NJ, USA: Wiley, 2010.

[33] M. Ameri, P. Ahmadi, and A. Hamidi, "Energy, exergy and exergoeconomic analysis of a steam power plant: A case study," *Int. Journal of Energy Research*, vol. 33, no. 5, pp. 499–512, Apr. 2009.

[34] M. K. Manesh, S. K. Abadi, M. Amidpour, and M. H. Hamedi, "A new targeting method for estimation of cogeneration potential and total annualized cost in process industries," *Chemical Engineering Research and Design*, vol. 91, no. 6, pp. 1039–1049, Jun. 2013.

[35] R. T. Marler and J. S. Arora, "The weighted sum method for multi-objective optimization: New insights," *Structural and Multidisciplinary Optimization,* vol. 41, no. 6, pp. 853–862, Jun. 2010.

[36] I. H. Aljundi, "Energy and exergy analysis of a steam power plant in Jordan," *Applied Thermal Engineering,* vol. 29, no. 2-3, pp.324–328, Feb. 2009.

[37] A. Mohammad, A. Pouria, H. Armita, "Energy, exergy and exergoeconomic analysis of a steam power plant: A case study," *Int. Journal of Energy Research,* vol. 33, pp. 499–512, 2009.